Supplementary Materials

The Molecular Structure of a Phosphatidylserine Bilayer Determined by Scattering and Molecular Dynamics Simulations

Jianjun Pan[1]*, Xiaolin Cheng[2,3], Luca Monticelli[4,5], Frederick A. Heberle[2], Norbert Kučerka[6,7], D. Peter Tieleman[8], John Katsaras[2,9,10] *

[1]Department of Physics, University of South Florida, Tampa, FL 33620, USA

[2]Oak Ridge National Laboratory, Oak Ridge, TN, 37831 USA

[3]Department of Biochemistry and Cellular and Molecular Biology, University of Tennessee, Knoxville, TN 37996, USA

[4]INSERM, UMR-S665, Paris, F-75015, France

[5]INTS, Paris, France

[6]Canadian Neutron Beam Centre, National Research Council, Chalk River, Ontario, Canada K0J 1J0

[7]Department of Physical Chemistry of Drugs, Faculty of Pharmacy, Comenius University, 832 32 Bratislava, Slovakia

[8]Department of Biological Sciences and Center for Molecular Simulation, University of Calgary, 2500 University Drive NW, Calgary, AB, Canada T2N 1N4

[9]Department of Physics and Astronomy, University of Tennessee, Knoxville, TN 37996, USA

[10]Joint Institute for Neutron Sciences, Oak Ridge National Laboratory, Oak Ridge, TN, 37831, USA

S1. Molecular volume of POPS lipid at different temperatures

For lipid volume measurements, 28.0 mg (m_L) of POPS powder was hydrated with 1.5 g (m_W) of 18MΩ.cm H_2O (Millipore) containing 100 mM NaCl. The lipid suspension was homogenized by repeated gentle vortexing and sonication in a water bath (45°C). The density of the lipid dispersion (ρ_s) was determined by a temperature controlled Anton-Paar DMA5000 (Graz, Austria) vibrating tube density meter. The density of the 100 mM NaCl buffer (ρ_W) was obtained using the same method. POPS' molecular volume was calculated as follows:

$$V_L = \frac{MW_L}{N_A m_L}\left(\frac{m_L + m_W}{\rho_S} - \frac{m_W}{\rho_W}\right), \tag{S1}$$

where MW_L is the molecular weight of POPS, and N_A is the Avagdro's number.
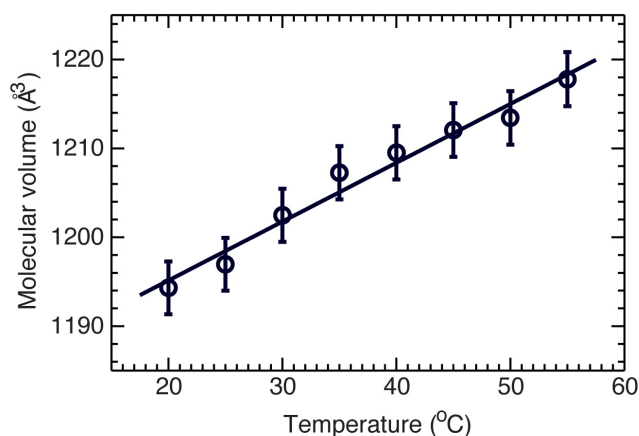
Fig. S1 Molecular volume of POPS as a function of temperature. Lipid volumes were obtained by measuring the solution density of POPS suspensions in 100 mM NaCl buffer using an Anton-Paar DMA5000 vibrating tube density meter. The solid line is a linear fit to the experimental data.

S2. Effect of buffer conditions

An important feature of POPS is the serine moiety in its headgroup. Exposure of the serine to the cell's extracellular side has been associated as a signal for programmed cell death. To study the effect of pH and salt concentration, we prepared POPS

unilamellar vesicles (ULVs) under three different buffer conditions, namely: (1) water; (2) water with pH=7.4; and (3) water with 100 mM NaCl and pH=7.4. The resulting SAXS data are shown in Fig. S2. It is clear that the three data sets overlap each other, indicating that the pH and salt concentration used have no measurable effect on POPS bilayer structure.

Serine's carboxylic moiety has a pKa of 2.21, while the pKa for its amino moiety is 9.15. The typical pH value for pure water is 6.0-8.5. Not unexpectedly, titration to pH=7.4 has no effect on serine's charge state. This is consistent with the observation that regardless of buffer used, POPS bilayer structure did not change. The negligible effect imparted by 100 mM NaCl can be understood by the fact that POPS is made in the sodium salt form. If the intrinsic amount of sodium salt is sufficient for the lipid to form all possible lipid-ion interactions, then the addition of 100 mM NaCl will have no impact. Another possible explanation is that, lipid-ion interactions do not affect POPS bilayer structure.
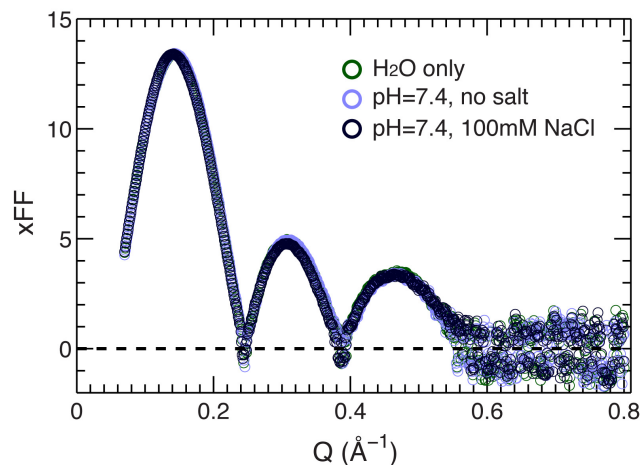
Fig. S2 Effects of pH and salt concentration on POPS bilayer structure. The X-ray form factors of a POPS bilayer were obtained at three buffer conditions: (1) H_2O only; (2) pH=7.4 with 5mM HEPES; and (3) pH=7.4 with 5mM HEPES and 100 mM NaCl.

S3. Small-angle neutron scattering

SANS data were taken at the Spallation Neutron Source (SNS) EQ-SANS and High Flux Isotope Reactor (HFIR) Bio-SANS instruments located at the Oak Ridge National Laboratory. For EQ-SANS experiments, time-of-flight data were obtained by using a truncated white beam (wavelength λ of 2.5-6.0 Å) and a sample-to-detector distance of 2.0 m. The resultant scattering vector Q covered a range from 0.03 to 0.8 Å^{-1} [$Q = 4\pi\sin(\theta)/\lambda$, where 2θ is the scattering angle with respect to the incident beam]. For Bio-SANS experiments, steady-state data were obtained using a fixed wavelength neutron beam (λ of 6.0 Å with a 15% wavelength dispersion) and a detector-to-sample distance of 1.4 m, resulting in Q ranging from 0.03 to 0.4 Å^{-1}. Both the time-of-flight and steady-state SANS data were reduced and background corrected using the Mantid software provided by the facility (http://www.mantidproject.org/). For data analysis, the reduced scattering intensity I was converted into a neutron form factor (nFF) following $nFF = Q \times \text{sign}(I) \times \sqrt{|I|}$, where sign($I$) refers to the sign of I (*i.e.*, plus or minus for positive and negative intensities, respectively). It was observed that SANS data from the two instruments were the same, within experimental uncertainties, and there was no usable scattering signal beyond $Q = 0.3$ Å^{-1}. For clarity, only Bio-SANS data between 0.05 and 0.3 Å^{-1} were used for bilayer structure analysis.

S4. Small-angle X-ray scattering

SAXS data were collected at the Cornell High Energy Synchrotron Source G-1 station. ULV samples in different buffer solutions were loaded into 1.5mm-diameter quartz capillaries, which were then placed in a temperature controlled, multi-position sample holder. A collimated X-ray source with a 1.17 Å wavelength and a sample-to-detector distance of 426.7 mm was used (calibrated with silver behenate). The isotropic SAXS data were collected using a 1024×1024 pixel array FLICAM charge-coupled device, and radially averaged into a one-dimensional intensity I profile, which was corrected for background and converted into an X-ray form factor xFF using the same mathematical relationship as was used for the SANS data. Of note are the negative and positive values of xFF at $Q > 0.6$ Å^{-1} (Fig. 1). They are the result of the Gaussian

distribution of the scattering intensities, which are centered about zero. The form factor, therefore, has an equal probability of assuming either a positive or negative value.

S5. SDP model of a POPS bilayer

The experimental POPS bilayer structure was determined by jointly refining SANS and SAXS data using the scattering density profile (SPD) model analysis. Similar to the reported phosphatidylcholine (PC) and phosphatidylglycerol (PG) bilayers [1-5], SDP model analysis for the PS bilayer requires parsing the PS lipid molecule into distinct groups, depending on their scattering characteristics (example is shown in Fig. 1). The POPS bilayer was parsed into six components (Fig. 1A). Specifically, the headgroup was divided into the glycerol-carbonyl backbone (G1, firebrick), phosphate (G2, magenta), and terminal serine (G3, green) groups. The hydrocarbon chain was described by the terminal methyl (CH3, marine), methylene (CH2, cyan) and methine (CH, orange) groups. Figure 1B shows a parsed POPS lipid molecule. The number density distribution of each component, $P_i(z)$, is shown in Fig. 1C. $P_i(z)$ was calculated by summing the number of total non-hydrogen atoms of component i within a bin of $\Delta z = 0.2$ Å, and then normalized by the area of the simulation box. Assuming there is no persistent vacancy within the system—an assumption supported by MD simulations—the component volume V_i can be obtained by solving an array of linear equations at every z [6]:

$$\sum_i V_i \times P_i(z) = \sum_i vP_i(z) = 1, \tag{S2}$$

where $vP_i(z)$ is the component volume probability (Fig. 1D). It is clear that the volume probability of the G1, G2, G3, CH and CH3 groups can be well described by Gaussian functions:

$$vP_i = \frac{V_i}{A\sqrt{2\pi}\sigma_i}\left\{\exp\left[-\frac{(z-z_0)^2}{2\sigma_i^2}\right] + \exp\left[-\frac{(z+z_0)^2}{2\sigma_i^2}\right]\right\}, \tag{S3}$$

where z_{0i} and σ_i are the Gaussian center and width of component i. The total hydrocarbon chain region can be well described by the subtraction of two error functions. Therefore, the volume probability of the CH2 component can be obtained by:

$$vP_{CH2} = \frac{1}{2}\left[\text{erf}\left(\frac{z + z_{HC}}{\sqrt{2}\sigma_{HC}} \right) - \text{erf}\left(\frac{z - z_{HC}}{\sqrt{2}\sigma_{HC}} \right) \right] - vP_{CH}(z) - vP_{CH3}(z), \quad\quad (S4)$$

$$\text{erf}(z) = \frac{2}{\sqrt{\pi}} \int_0^z \exp\left(-t^2\right)dt \ , \quad\quad (S5)$$

where z_{HC} is the half length of the bilayer hydrocarbon chain, and σ_{HC} describes the width of the error function's transition region. After obtaining the volume probabilities for the different lipid components, the water volume probability can be obtained using $vP_{water}(z) = 1 - \sum_{i=lipid} vP_i$, i.e., the water volume probability complements that of the lipid.

The X-ray (or neutron) SDP for each component $\rho_i(z)$ is the product of the component volume probability $vP_i(z)$ and the component's total number of electrons (or neutron scattering lengths). The model X-ray (or neutron) form factor is obtained from the Fourier transform of the summation of the component X-ray (or neutron) SDPs, minus the solvent's electron (or neutron scattering length) density, described mathematically as:

$$FF(\text{model}, Q) = \frac{1}{2\pi} \int_{-\infty}^{\infty} \left[\sum_i \rho_i(z) - \rho_{\text{water}} \right] \exp\left(-jQz\right)dz , \quad\quad (S6)$$

where j is an imaginary number. The aim of SDP model analysis is to minimize the difference between the model form factors and the experimental X-ray and neutron form factors.

S6. Proton exchange of serine ammonium

Rapid proton exchange of solvent accessible ammonium hydrogens requires careful consideration of POPS' neutron scattering length density (NSLD) distribution as a function of solvent D_2O concentration. Two extreme cases are illustrated in Fig. S3. In 0% D_2O, three hydrogens are attached to the ammonium nitrogen in POPS' headgroup (Fig. S3A). Increasing the solvent D_2O concentration to 100% replaces the three hydrogens with three deuteriums (Fig. S3B), thus altering POPS's NSLD – hydrogen and deuterium have very different neutron scattering powers. Figure S3C shows the impact of proton exchange on NSLD distribution for a POPS bilayer in 100%D_2O. Compared to the cyan dashed line, proton exchange enhances NSLD in the headgroup region (orange solid line).
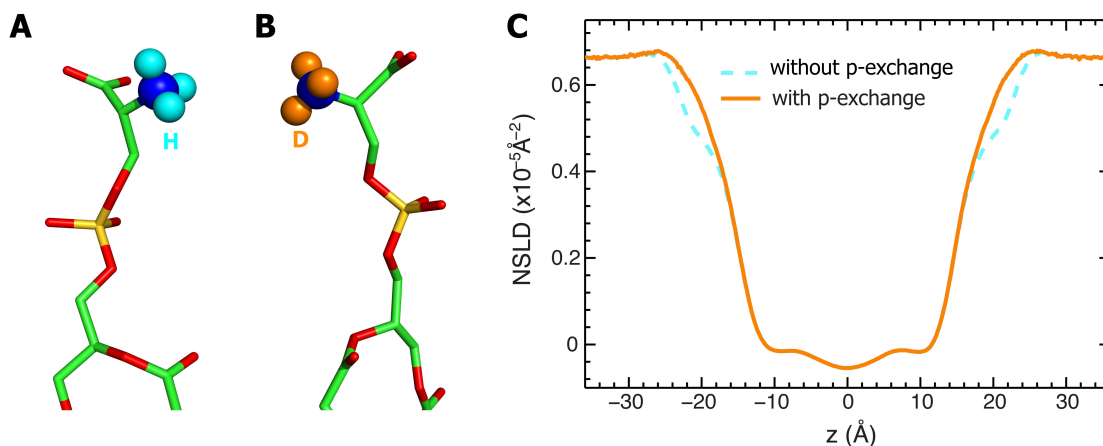
Fig. S3 The effect of proton exchange on POPS' neutron scattering power. (A) In 0% D_2O, three hydrogens (cyan spheres) are attached to the ammonium nitrogen (blue sphere). (B) In 100% D_2O, the three hydrogens are replaced by three deuteriums (orange spheres). (C) The NSLD distribution for a POPS bilayer in 100% D_2O. The cyan dashed line was obtained by assuming no exchange of the three ammonium hydrogens, while the solid orange line was obtained after taking proton exchange into account. As discussed in the main text, the bilayer NSLD was obtained from atom number density distributions (NAP_nT simulations with lipid area fixed at 62.0 $Å^2$) after being multiplied by their corresponding neutron scattering powder.

S7. SDP model analysis using two Gaussian functions to describe a POPS headgroup
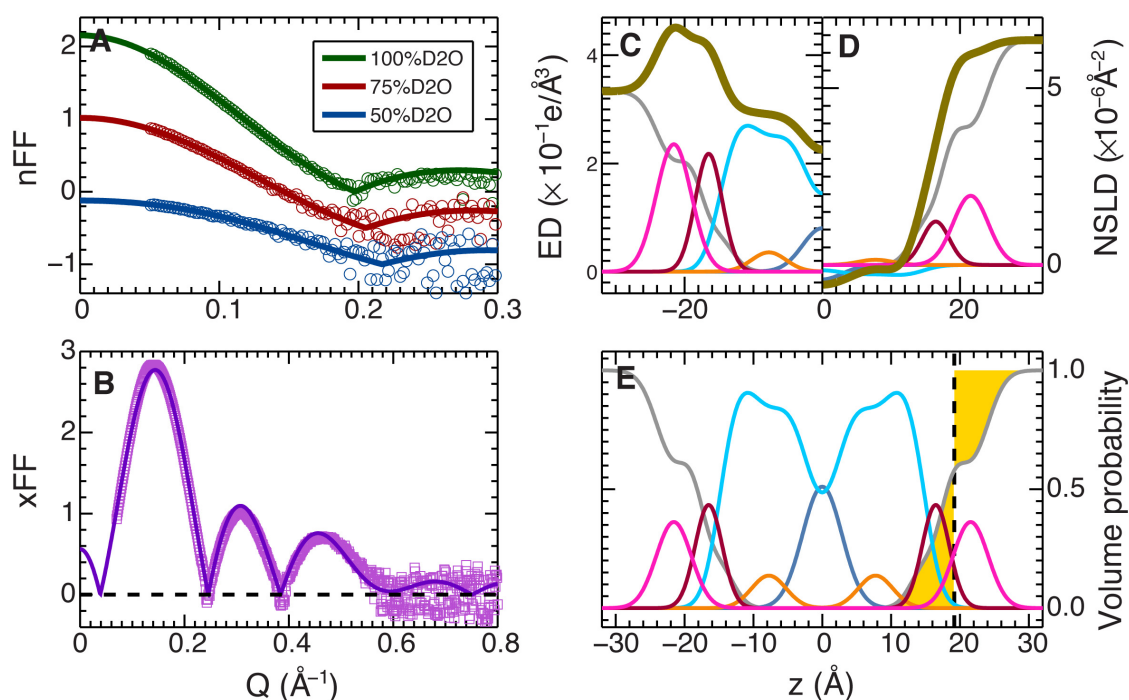
Fig. S4 SDP model analysis using two Gaussian functions to represent POPS headgroup. The resulting lipid area is 62.5 Å^2, compared to 62.7 Å^2 when the headgroup is described by three Gaussian functions.

References

1. N. Kučerka, J. F. Nagle, J. N. Sachs, S. E. Feller, J. Pencer, A. Jackson and J. Katsaras, *Biophys. J.*, 2008, **95**, 2356-2367.
2. N. Kučerka, M. P. Nieh and J. Katsaras, *BBA-Biomembranes*, 2011, **1808**, 2761-2771.
3. J. J. Pan, F. A. Heberle, S. Tristram-Nagle, M. Szymanski, M. Koepfinger, J. Katsaras and N. Kucerka, *BBA-Biomembranes*, 2012, **1818**, 2135-2148.
4. F. A. Heberle, J. J. Pan, R. F. Standaert, P. Drazba, N. Kucerka and J. Katsaras, *Eur. Biophys. J. Biophy.*, 2012, **41**, 875-890.
5. N. Kučerka, B. W. Holland, C. G. Gray, B. Tomberli and J. Katsaras, *J. Phys. Chem. B*, 2012, **116**, 232-239.
6. H. I. Petrache, S. W. Dodd and M. F. Brown, *Biophys. J.*, 2000, **79**, 3172-3192.